THE JOURNAL OF BIOLOGICAL CHEMISTRY
Vol. 279, No. 50, Issue of December 10, pp. 52772–52780, 2004
Printed in U.S.A.
© 2004 by The American Society for Biochemistry and Molecular Biology, Inc.

Cholesterol and 25-Hydroxycholesterol Inhibit Activation of SREBPs by Different Mechanisms, Both Involving SCAP and Insigs*

Received for publication, September 8, 2004, and in revised form, September 23, 2004
Published, JBC Papers in Press, September 27, 2004, DOI 10.1074/jbc.M410302200

Christopher M. Adams‡§, Julian Reitz‡, Jef K. De Brabander¶, Jamison D. Feramisco‡‖, Lu Li‡, Michael S. Brown‡, and Joseph L. Goldstein‡ ‡‡**

From the Departments of ‡Molecular Genetics and ¶Biochemistry, University of Texas Southwestern Medical Center, Dallas, Texas 75390-9046

The current paper demonstrates that cholesterol and its hydroxylated derivative, 25-hydroxycholesterol (25-HC), inhibit cholesterol synthesis by two different mechanisms, both involving the proteins that control sterol regulatory element-binding proteins (SREBPs), membrane-bound transcription factors that activate genes encoding enzymes of lipid synthesis. Using methyl-β-cyclodextrin as a delivery vehicle, we show that cholesterol enters cultured Chinese hamster ovary cells and elicits a conformational change in SREBP cleavage-activating protein (SCAP), as revealed by the appearance of a new fragment in tryptic digests. This change causes SCAP to bind to Insigs, which are endoplasmic reticulum retention proteins that abrogate movement of the SCAP·SREBP complex to the Golgi apparatus where SREBPs are normally processed to their active forms. Direct binding of cholesterol to SCAP in intact cells was demonstrated by showing that a photoactivated derivative of cholesterol cross-links to the membrane domain of SCAP. The inhibitory actions of cholesterol do not require the isooctyl side chain or the Δ5-double bond of cholesterol, but they do require the 3β-hydroxyl group. 25-HC is more potent than cholesterol in eliciting SCAP binding to Insigs, but 25-HC does not cause a detectable conformational change in SCAP. Moreover, a photoactivated derivative of 25-HC does not cross-link to SCAP. These data imply that cholesterol interacts with SCAP directly by inducing it to bind to Insigs, whereas 25-HC works indirectly through a putative 25-HC sensor protein that elicits SCAP-Insig binding.

Nearly 30 years ago, during early studies of feedback inhibition of cholesterol synthesis in cultured cells, it was noted that oxygenated sterols such as 25-hydroxycholesterol were more than 50-fold more potent than cholesterol in reducing the activity of 3-hydroxy-3-methylglutaryl-CoA reductase, the rate-controlling enzyme in cholesterol biosynthesis (1–4). These experiments were conducted by dissolving sterols in ethanol and adding them to protein-containing aqueous culture media in which cholesterol forms an amorphous suspension and thus has poor access to the interior of the cell. When cholesterol was delivered to cells in low density lipoprotein (LDL),[1] a physiologic carrier that enters cells through LDL receptors, the ability of cholesterol to suppress 3-hydroxy-3-methylglutaryl-CoA reductase was enhanced (5). Later, when methods were devised to reconstitute LDL with sterol esters, it was observed that 25-hydroxycholesterol was only about 5-fold more potent than cholesterol when both sterol esters were reconstituted into LDL and delivered through LDL receptors (6). The question of whether cholesterol itself is a regulator or whether it must be converted to an oxygenated metabolite, like 25-hydroxycholesterol, remained unresolved (7). In view of this ambiguity, studies of feedback regulation in our laboratory have generally used a mixture of cholesterol and 25-hydroxycholesterol in a 10:1 molar ratio added in ethanol.

In recent years the mechanism of sterol feedback regulation at the transcriptional level has been elucidated, but the issue of 25-hydroxycholesterol *versus* cholesterol as a physiologic regulator remains unsettled. Transcriptional regulation is mediated by sterol regulatory element-binding proteins (SREBPs), a three-member family of membrane-bound transcription factors (8). The NH_2-terminal domains of SREBPs are transcription factors of the basic helix-loop-helix-leucine zipper variety. This domain is followed by a membrane attachment domain consisting of two transmembrane helices, which is followed by a COOH-terminal regulatory domain. SREBPs are oriented in endoplasmic reticulum (ER) membranes in a hairpin fashion with their NH_2-terminal and COOH-terminal domains facing the cytosol. Immediately after synthesis, SREBPs form a complex with SREBP cleavage-activating protein (SCAP), a polytopic ER protein with eight membrane-spanning helices. In sterol-depleted cells, SCAP escorts its bound SREBP to the Golgi apparatus where the SREBP is processed sequentially by two membrane-embedded proteases that release the NH_2-terminal domain so that it can enter the nucleus where it activates transcription of the gene encoding 3-hydroxy-3-methylglutaryl-CoA reductase and more than 30 other genes whose products are necessary for lipid synthesis (9, 10). When 25-hydroxycholesterol is delivered to cells in ethanol or when

* This work was supported by Grant HL20948 from the National Institutes of Health and grants from the Perot Family Foundation and the W. M. Keck Foundation. The costs of publication of this article were defrayed in part by the payment of page charges. This article must therefore be hereby marked "*advertisement*" in accordance with 18 U.S.C. Section 1734 solely to indicate this fact.

§ Supported by the Physician Scientist Training Program of the University of Texas Southwestern Medical Center.

‖ Supported by National Institutes of Health Medical Scientist Training Grant GM-08014.

** To whom correspondence may be addressed: Dept. of Molecular Genetics, University of Texas Southwestern Medical Center, 5323 Harry Hines Blvd., Dallas, TX 75390-9046. E-mail: mike.brown@utsouthwestern.edu.

‡‡ To whom correspondence may be addressed: Dept. of Molecular Genetics, University of Texas Southwestern Medical Center, 5323 Harry Hines Blvd., Dallas, TX 75390-9046. E-mail: joe.goldstein@utsouthwestern.edu.

[1] The abbreviations used are: LDL, low density lipoprotein; ER, endoplasmic reticulum; 25-HC, 25-hydroxycholesterol; photo 25-HC, 6-azi-5α-cholestan-3β,25-diol; MCD, methyl-β-cyclodextrin; OSBP, oxysterol-binding protein; PBS, phosphate-buffered saline; photocholesterol, 6-azi-5α-cholestan-3β-ol; PNGase F, peptide *N*-glycosidase F; siRNA, small interfering RNA; SCAP, SREBP cleavage-activating protein; SREBP, sterol regulatory element-binding protein; TM, transmembrane helix; CHO, Chinese hamster ovary; Tricine, *N*-[2-hydroxy-1, 1-bis(hydroxymethyl)ethyl]glycine; HSV, herpes simplex virus.

This paper is available on line at http://www.jbc.org

This is an Open Access article under the CC BY license.

cholesterol is delivered in LDL, SCAP becomes trapped in the ER. The bound-SREBP is no longer carried to the Golgi apparatus, and the NH_2-terminal domain cannot enter the nucleus (11). As a result, transcription of the lipid biosynthetic genes declines.

Retention of the SCAP·SREBP complex in the ER is mediated by the sterol-induced binding of SCAP to Insigs, which are resident proteins of the ER membrane (11, 12). Cultured cells express two Insig isoforms, designated Insig-1 and Insig-2, that are closely related in amino acid sequence and have the same membrane topology (13). When mixtures of cholesterol and 25-hydroxycholesterol are added to cultured cells, SCAP is induced to bind to Insig-1 and Insig-2, as revealed by co-immunoprecipitation experiments and by detection of the complex by blue native gel electrophoresis (11, 12). Mutant forms of SCAP harboring any one of three point mutations fail to bind Insig-1 and Insig-2, and thus they constitutively transport SREBPs to the Golgi even in the presence of sterols (11, 14).

The mechanism by which cholesterol regulates SCAP·Insig binding was disclosed recently by studies demonstrating that SCAP directly binds cholesterol (15) and thereby undergoes a conformational change that allows it to bind to Insigs (16). In one set of experiments, we isolated sealed ER membrane vesicles from cholesterol-depleted cells, taking advantage of the observation that cholesterol can be solubilized by methyl-β-cyclodextrin (MCD) in a form that allows it to partition into membranes (17). We incubated the cholesterol-depleted membranes with cholesterol·MCD complexes and then digested them with trypsin. The digests were subjected to electrophoresis in SDS-polyacrylamide gels and blotted with an antibody against the luminal loop that lies between transmembrane segments 7 and 8 of SCAP (18). In membranes from sterol-depleted cells, trypsin cut at arginines 496 and 747, generating a fragment of 37 kDa. When the membranes were treated with cholesterol·MCD, a previously sequestered arginine at position 503 was exposed, and trypsin cleavage gave a smaller product of 35 kDa (16, 19). This cholesterol-induced conformational change in SCAP was enhanced when cells expressed excess Insigs, and this increase was not seen with the sterol-resistant SCAP mutants that do not bind Insigs (16). The suggestion that this conformational change reflects direct binding of cholesterol to SCAP was supported strongly by the recent finding that the purified, detergent-solubilized membrane domain of SCAP binds [^{3}H]cholesterol with stereospecificity and saturation kinetics (15). Competition experiments revealed that binding required the 3β-hydroxyl group of cholesterol, but it did not require the side chain (15).

Although the above-cited studies provide a mechanism for feedback regulation by cholesterol, they raise questions about whether 25-hydroxycholesterol acts by the same mechanism. Indeed, in the direct binding studies, SCAP failed to bind 25-hydroxycholesterol (15). Moreover, 25-hydroxycholesterol did not induce a conformational change in SCAP when added to membranes *in vitro* (16).

In the current studies, we use a variety of methods to demonstrate that cholesterol acts in intact cells by binding to SCAP and inducing a conformational change, whereas 25-hydroxycholesterol neither binds nor induces a conformational change. Nevertheless, both sterol regulators block SREBP processing by inducing SCAP to bind to Insig. These studies strongly suggest that cells must contain another protein that recognizes 25-hydroxycholesterol and thereby induces SCAP to bind to Insigs.

EXPERIMENTAL PROCEDURES

Materials—We obtained sterols from Steraloids, Inc.; MCD and hydroxypropyl-β-cyclodextrin from Cyclodextrin Technologies Development, Inc.; trypsin (type 1 from bovine pancreas), soybean trypsin inhibitor, chymotrypsin, and Triton X-100 from Sigma; peptide *N*-glycosidase F (PNGase F) from New England Biolabs, Inc.; Nonidet P-40 Alternative from Calbiochem; and FuGENE 6 reagent from Roche Applied Science. Complexes of sterols with MCD were prepared as previously described (19). Lipoprotein-deficient serum ($d > 1.215$ g/ml) was prepared by ultracentrifugation (20). Solutions of sodium mevalonate and compactin were prepared as previously described (21). Solutions of sodium oleate were prepared as previously described (20).

Chemical Syntheses—6-Azi-5α-cholestan-3β-ol (photocholesterol) was prepared from 6-keto-5α-cholestan-3β-ol as previously described (22). 6-Azi-5α-cholestan-3β,25-diol (photo 25-hydroxycholesterol) was prepared similarly from 6-keto-5α-cholestan-3β,25-diol. The latter compound was prepared by a modification of the method of Tavares *et al.* (23). In brief, 25-HC (1 g) was treated with *t*-butyldiphenylsilyl chloride (2.8 equivalents) and imidazole (6.4 equivalents) in dimethylformamide (0.07 M) for 16 h at room temperature. After extractive work-up and chromatographic purification, the corresponding silylether was obtained in 74% yield (1.2 g). This material was dissolved in dry tetrahydrofuran (0.06 M) and treated with a 1 M BH_3 solution in tetrahydrofuran (3.8 equivalents). After stirring for 48 h at room temperature, the resulting solution was added to a solution of pyridinium chlorochromate (10 g) in dichloromethane (150 ml). After refluxing for 1 h, the mixture was filtered over florisil, and the filtrate was concentrated and purified by silica gel chromatography to provide 1.04 g (85%) of the corresponding 6-keto derivative. 6-Keto-5α-cholestan-3β,25-diol was obtained by deprotection of the silylether with tetrabutylammonium fluoride (2.6 equivalents) in tetrahydrofuran (0.17 M). Extraction and purification by silica gel chromatography provided 0.6 g of pure 6-keto-5α-cholestan-3β,25-diol (90% yield).

Plasmids—The following plasmids have been described previously. pCMV-SCAP, pCMV-SCAP(D443N), pCMV-SCAP(Y298C), and pCMV-SCAP(L315F) encode wild type and mutant versions of hamster SCAP under control of the cytomegalovirus promoter (14, 18). pCMV-Insig1-Myc and pCMV-Insig2-Myc encode human Insig-1 and Insig-2, respectively, with six tandem copies of the c-Myc epitope tag at their COOH termini (11, 12). pTK-HSV-SREBP2 encodes human SREBP with an NH_2-terminal HSV epitope tag, under control of the thymidine kinase promoter (24). pTK-HSV-SCAP encodes wild type SCAP with two copies of the HSV epitope tag at the NH_2 terminus (25); and pCMV-CBP-FLAG-SCAP(TM1–6)-Myc encodes (5′ to 3′) a calmodulin-binding protein tag, a FLAG epitope, the first six transmembrane segments of hamster SCAP (amino acids 1–448), and three tandem copies of the c-Myc epitope (11).

Buffers—The following buffers were used: Buffer A contains 50 mM Hepes-KOH, pH 7.4, 250 mM sucrose, 10 mM KCl, 1.5 mM $MgCl_2$, 5 mM sodium EGTA, 5 mM sodium EDTA. Buffer B contains 10 mM Tris-HCl, pH 7.6, 100 mM NaCl, 1% (w/v) SDS, and protease inhibitor mixture (25 μg/ml *N*-acetyl-leucinal-leucinal-norleucinal, 1 μg/ml pepstatin A, 2 μg/ml aprotinin, 10 μg/ml leupeptin, 200 μM phenylmethylsulfonyl fluoride). Buffer C contains 20 mM Hepes-KOH, pH 7.6, 25% (v/v) glycerol, 0.42 M NaCl, 1.5 mM $MgCl_2$, 1 mM sodium EDTA, 1 mM sodium EGTA, and protease inhibitor mixture. Buffer D contains 250 mM Tris-HCl, pH 6.8, 10% SDS, 25% glycerol, 0.2% (w/v) bromphenol blue, and 5% (v/v) 2-mercaptoethanol. Buffer E contains 40 mM Hepes-KOH, pH 7.4, 2 mM magnesium acetate, and protease inhibitor mixture.

Tissue Culture Media—Medium A is a 1:1 mixture of Ham's F-12 medium and Dulbecco's modified Eagle's medium containing 100 units/ml penicillin and 100 μg/ml streptomycin sulfate. Medium B is medium A supplemented with 5% (v/v) fetal calf serum. Medium C is medium B supplemented with 5 μg/ml cholesterol, 1 mM sodium mevalonate, and 20 μM sodium oleate. Medium D is medium A supplemented with 5% newborn calf lipoprotein-deficient serum, 50 μM sodium compactin, and 50 μM sodium mevalonate. Medium E is medium D supplemented with 1% (w/v) hydroxypropyl-β-cyclodextrin. Medium F is Dulbecco's modified Eagle's medium (low glucose) containing 100 units/ml penicillin and 100 μg/ml streptomycin sulfate.

Cell Culture—Chinese hamster ovary (CHO) K1 cells and SRD-13A cells (a SCAP null mutant clone derived from γ-irradiated CHO-7 cells (26)) were grown in monolayer at 37 °C in an atmosphere of 8–9% CO_2 and maintained in medium B and medium C, respectively. SV-589 cells (an immortalized line of human fibroblasts expressing the SV40 large T antigen (27)) were grown in monolayer at 37 °C in 5% CO_2 and maintained in medium F supplemented with 10% fetal calf serum.

Analysis of SREBP Processing in CHO Cells—On day 0, the cells were set up for experiments in medium B at 7×10^5 cells/100-mm dish. On day 1, the cells were washed twice with phosphate-buffered saline (PBS), and switched to medium D or medium E for varying times of incubation as described in the figure legends. Following incubation, the

cells were washed once with cold PBS, then treated with 500 μl of buffer B, and scraped into 1.5-ml tubes on ice. The cells were passed through a 22-gauge needle 11 times and then shaken for 20 min at room temperature using a Vortex Genie 2 (Fisher). The protein concentration of each total cell extract was measured (BCA kit; Pierce) after which an aliquot of cell extract (25 μg) was mixed with 0.25 volume of buffer D, heated for 7 min at 95 °C, and then subjected to 8% SDS-PAGE and immunoblot analysis.

Transient Transfection and Fractionation of SRD-13A Cells—On day 0, the cells were set up for experiments in medium C at 7.5×10^5 cells/100-mm dish. On day 2, the cells were transfected in medium B with plasmids by using FuGENE 6 reagent as described (26). The total amount of DNA in each transfection was adjusted to 4–7 μg/dish by the addition of pcDNA3 mock vector. After incubation at 37 °C for 24 h, the cells were washed twice with PBS and switched to medium D or medium E for varying times of incubation as described in the figure legends. The cells were harvested, and nuclear extracts in buffer C (28) and 20,000 × *g* membrane fractions in buffer A (19) were prepared as described in the indicated reference.

Blue Native-PAGE for Detection of SCAP·Insig-1 Complex—Aliquots of the 20,000 × *g* membrane fraction were resuspended in buffer E containing 0.4% (w/v) Nonidet P-40 Alternative and then mixed with an equal volume of buffer E containing no detergent. After incubation on ice for 30 min, detergent-insoluble material was removed by centrifugation at $1 \times 10^5 \times g$ for 30 min at 4 °C. The samples were then analyzed by 4–16% blue native-PAGE as described (11).

Sterol Treatment of Membranes in Vitro—Aliquots (100 μg) of the 20,000 × *g* membrane fraction were resuspended in buffer A with or without sterol·MCD complex to give a final volume of 500 μl. The mixture was incubated at room temperature for 20 min and then centrifuged at 20,000 × *g* at 4 °C for 10 min. Buffer was aspirated from the resulting membrane pellets, and the membranes were resuspended in buffer A for subsequent photoaffinity labeling and/or protease treatment.

Photoaffinity Labeling—All of the experiments using photoactive sterols were performed in the dark. Irradiation of membranes *in vitro* was performed using a portable ultraviolet lamp (UVP model UVL-28, peak transmission at 365 nm) applied to the samples contained in 1.5-ml tubes on ice for 10–15 min. Irradiation of intact transfected SRD-13A cells used a GE Black light bulb (model F40BLB) placed at a distance of 11 cm from open 100-mm dishes of cells for 20 min at room temperature.

Proteolytic Cleavage of SCAP—Our previously described protocol (16, 19) was modified as follows. Aliquots (100 μg) of the 20,000 × *g* membrane fraction from transfected SRD-13A cells were resuspended in 135 μl of buffer A. To each tube was added 2 μg of trypsin (in 5 μl), and the samples were incubated at 30 °C for 30 min. Trypsin digestion was stopped by the addition of 100 μg of soybean trypsin inhibitor (in 5 μl). PNGase F treatment, acetone precipitation, and resuspension in buffer D were performed as described (19). In experiments using chymotrypsin, 50 μg of membranes were resuspended in buffer A containing 1% Triton X-100 and 30 μg of chymotrypsin to give a final volume of 68 μl. The samples were incubated at 30 °C for 30 min and then moved to ice for 10 min before mixing with 14 μl of buffer D and heating at 95 °C for 5 min. Trypsin-treated samples and chymotrypsin-treated samples were analyzed on 12 or 15% Tris-Tricine gels, respectively, except as noted in the legend to Fig. 9*B*.

RNA Interference—Single-stranded small interfering RNAs (siRNAs) were synthesized by the University of Texas Southwestern RNA Oligonucleotide Synthesis Core. Complementary single-stranded siRNAs were annealed into duplexes at a final concentration of 20 μM. The oligonucleotides used to generate duplex siRNA (sense/antisense) were as follows: human Insig-1, UGGUGUCUAUCAGUAUACATT/UGUAUACUGAUAGACACCUTT and CCAGUGCUAAAUUGGAUUUTT/AAAUCCAAUUUAGCACUGGTT; human Insig-2, UCUCCAGAUUUCCUCUAUGTT/CAUAGAGGAAAUCUGGAGATT and GUGCUAAAGUGGAUUUCGATT/UCGAAAUCCACUUUAGCACTT; and green fluorescent protein, CAGCCACAACGUCUAUAUCTT/GAUAUAGACGUUGUGGCUGTT.

On day 0, SV-589 cells were set up at a density of 1.75×10^5 cells/100-mm dish in medium F supplemented with 10% fetal calf serum. On day 1, the cells were washed once with 8 ml of PBS, refed with 3 ml of medium F (without antibiotics), and then transfected with siRNA using a ratio of 10 μl of OligofectAMINE™ reagent (Invitrogen) to 1050 pmol of siRNA duplexes/dish (added in a volume of 1 ml) as described by the manufacturer. After incubation at 37 °C for 4 h, the cells received additional medium to give a final volume of 7 ml of medium F containing fetal calf serum at a final concentration of 10%. On day 4, after incubation for 3 days, the cells were used for experiments. Quantification of cellular mRNAs targeted for knockdown was done by real time PCR (29).

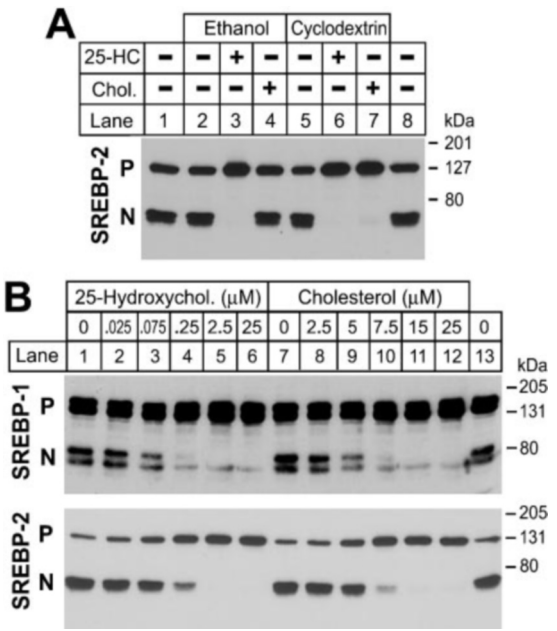

FIG. 1. **Sterol-mediated inhibition of SREBP processing in CHO cells.** *A*, CHO K1 cells were incubated at 37 °C in medium E for 1 h and then for 6 h in medium D in the absence or presence of 25-HC or cholesterol (*Chol.*) as indicated. Both sterols were tested at a concentration of 25 μM and were added to the medium from stock solutions containing either 25 mM sterol in ethanol (*lanes 2–4*) or 2.5 mM sterol complexed to 25 mM MCD in water (*lanes 5–7*). The medium for cells in *lanes 1* and *8* received neither ethanol nor MCD. After the last incubation, the cells were harvested, and total cell extracts were subjected to SDS-PAGE followed by immunoblot analysis with IgG-7D4 (anti-SREBP-2). *P* and *N* denote the uncleaved membrane precursor and cleaved nuclear forms of SREBP-2, respectively. *B*, CHO K1 cells were incubated for 1 h in medium E and then for 6 h in medium D containing varying concentrations of 25-HC/MCD (*lanes 1–6*) or cholesterol/MCD (*lanes 7–12*). Total cell extracts were analyzed by immunoblot with antibodies against SREBP-2 (monoclonal IgG-7D4) or SREBP-1 (polyclonal antiserum). *A* and *B*, filters were exposed to film for 30 s.

Immunoblot Analysis—After SDS-PAGE electrophoresis, the proteins were transferred to Hybond-C extra nitrocellulose filters (Millipore). The immunoblots were performed at room temperature using the following primary antibodies: 5 μg/ml of IgG-7D4, a mouse monoclonal antibody against the NH_2 terminus of hamster SREBP-2 (30); 5 μg/ml of IgG-9D5, a mouse monoclonal antibody against hamster SCAP (18); 5 μg/ml of IgG-1D2, a mouse monoclonal antibody against the NH_2 terminus of human SREBP-2 (12); 1 μg/ml of IgG-9E10, a mouse monoclonal antibody against c-Myc (11); a 1:15,000 dilution of IgG-HSV-Tag (Novagen); and a 1:5,000 dilution of a rabbit polyclonal antiserum 181 against the NH_2 terminus of hamster SREBP-1c. This latter antibody (previously undescribed) was prepared by immunizing rabbits with a bacterially produced and purified fusion protein encoding an NH_2-terminal His_6 tag, followed by amino acids 1–125 of hamster SREBP-1c (31). For all of the immunoblot analyses, the bound antibodies were visualized by chemiluminescence (SuperSignal Substrate; Pierce) using a 1:5,000 dilution of anti-mouse IgG (Jackson Immunoresearch Laboratories, Inc.) or a 1:2,000 dilution of anti-rabbit IgG (Amersham Biosciences) conjugated to horseradish peroxidase. The filters were exposed to Kodak X-Omat Blue XB-1 film at room temperature.

RESULTS

Fig. 1*A* compares the effects of cholesterol and 25-HC on processing of endogenous SREBP-2 in CHO cells when each sterol was either dissolved in ethanol or complexed to MCD and then added to the culture medium for 6 h. When sterols were omitted from the medium, ~50% of SREBP-2 was found in the cleaved nuclear form (*lanes 1*, *2*, *5*, and *8*). When added in ethanol to achieve a final concentration of 25 μM, 25-HC inhibited SREBP-2 processing (*lane 3*), but cholesterol dissolved in

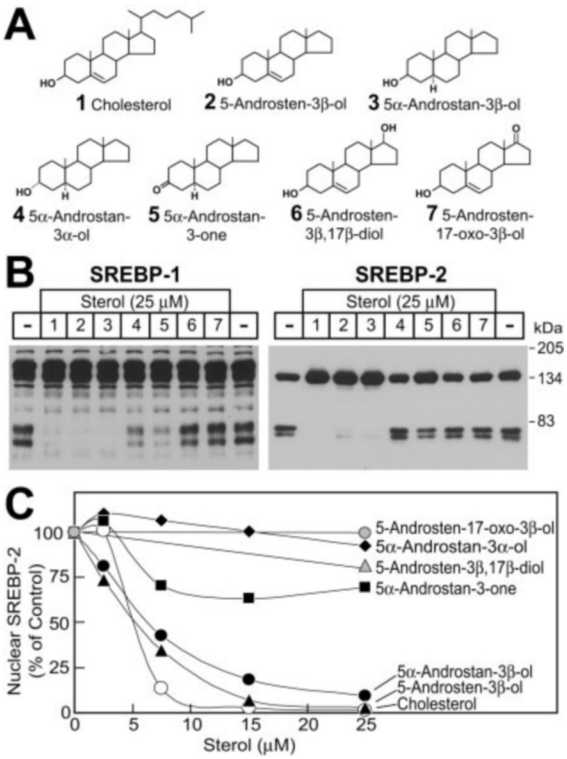

FIG. 2. **Structure-function analysis of sterol inhibition of SREBP processing in CHO cells.** *A*, structures of sterols tested. *B*, immunoblot analysis of SREBP-1 and SREBP-2. CHO K1 cells were incubated for 1 h in medium E and then for 6 h in medium D containing 25 μM of the indicated sterol complexed to MCD. Total cell extracts were immunoblotted for SREBP-1 and -2 as described in the legend to Fig. 1*B*. The filters were exposed to film for 30 s. *C*, immunoblot analysis of SREBP-2. CHO K1 cells were incubated for 1 h in medium E and then for 6 h in medium D containing varying concentrations of the indicated sterol complexed to MCD. Total cell extracts were immunoblotted with IgG-7D4 (anti-SREBP-2), and the relative amount of nuclear SREBP-2 was quantified by densitometry and normalized to the value in cells receiving no sterols ("100% of control").

ethanol had no effect (*lane 4*). In contrast, when the sterols were delivered as a complex with MCD and added to achieve the same 25 μM concentration, both 25-HC and cholesterol suppressed SREBP-2 cleavage (*lanes 6* and *7*). SREBP-2 processing was not affected by the low concentrations of ethanol or MCD used to deliver the sterols (compare *lanes 2* and *5* with *lanes 1* and *8*). The dose responses to 25-HC·MCD and cholesterol·MCD are shown in Fig. 1*B*. 25-HC·MCD partially inhibited processing of both SREBP-1 (*upper panel*) and SREBP-2 (*lower panel*) at a concentration of 0.25 μM, and it fully inhibited cleavage at 2.5 μM. Cholesterol·MCD was less potent, producing partial inhibition at 7.5 μM and nearly 100% inhibition at 15 μM.

To determine which structural features of cholesterol are required to inhibit SREBP processing, we tested several related sterols, each complexed to MCD (Fig. 2*A*). Prominent structural features of cholesterol (compound **1**) include the steroid nucleus, the 3-β hydroxyl group, the double bond at C-5–C-6, and the isooctyl side chain at C-17. Fig. 2 (*B* and *C*) shows that a sterol lacking the side chain (5-androsten-3β-ol; compound **2**), as well as a sterol lacking both the side chain and the double bond (5α-androstan-3β-ol; compound **3**), inhibited SREBP-1 and SREBP-2 processing with dose-response curves that were similar to that of cholesterol. Because sterols lacking the side chain inhibit SREBP processing, a side chain hydroxyl group is not required for the inhibitory effect of cholesterol. This finding supports the notion that cholesterol inhibits SREBP processing directly and not by conversion to a sterol

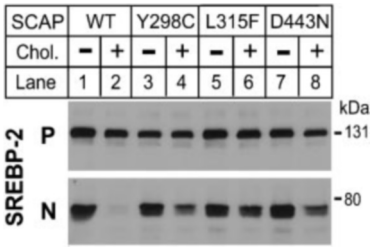

FIG. 3. **Cholesterol does not inhibit SREBP-2 processing in SCAP-deficient cells transfected with mutant SCAPs resistant to oxysterols.** SCAP-deficient SRD-13A cells were transfected with 2 μg of TK-HSV-SREBP-2, 0.6 μg of pCMV-Insig1-Myc, and 1.25 μg of the indicated wild type (*WT*) (*lanes 1* and *2*) or mutant pCMV-SCAP construct (*lanes 3–8*). After incubation for 24 h, the cells were incubated in medium E for 1 h and then for 8 h in medium D in the absence or presence of 25 μM cholesterol/MCD. The membrane and nuclear fractions were subjected to immunoblot analysis of SREBP-2 using anti-HSV IgG. The filters were exposed to film for 30 s (*upper panel*) and 2 min (*lower panel*). *P* and *N* denote the uncleaved membrane precursor and cleaved nuclear forms of SREBP-2, respectively.

with a hydroxyl at position 24, 25, or 27 in the side chain, all of which are known to be formed in cells (32).

The addition of a hydroxyl or a keto at the 17 position (compounds **6** and **7**) eliminated the suppressive effect of 5-androsten-3β-ol, suggesting that a polar group on the D ring actually inhibits activity. Although the side chain and the double bond were not required for activity, the 3β-hydroxyl group was crucial, because sterols with a 3α-hydroxyl group (5α-androstan-3α-ol; compound **4**) or a 3-keto group (5α-androstan-3-one; compound **5**) had only small effects on SREBP cleavage (Fig. 2, *B* and *C*).

When SCAP contains any one of three missense mutations (Y298C, L315F, or D443N), SREBP processing is resistant to inhibition by 25-HC (9, 14). To test whether these mutations render SREBP processing resistant to cholesterol, we transfected SCAP-deficient SRD-13A cells (26) with cDNAs encoding SREBP-2, Insig-1, and either wild type SCAP or one of the three SCAP mutants. Fig. 3 shows that cholesterol·MCD inhibited SREBP processing in cells expressing wild type SCAP (*lanes 1* and *2*), but it had little if any effect in cells expressing any one of the SCAP mutants (*lanes 3–8*). Inasmuch as these SCAP mutants prevent binding of SCAP to Insig-1 or Insig-2 (11, 12), these data suggest that Insig binding is required for cholesterol-mediated inhibition of SREBP processing.

Previous studies using both blue native-PAGE and co-immunoprecipitation showed that a combined mixture of 25-HC plus cholesterol stimulates the formation of complex between SCAP and Insig-1 or Insig-2 (11, 14). Fig. 4 shows a blue native-PAGE experiment designed to test the effect of either sterol alone on the SCAP·Insig-1 complex. To improve the signal-to-noise ratio of the blue native gels, we changed the detergent from digitonin, which we used previously (11), to 0.2% Nonidet P-40 Alternative (see "Experimental Procedures"). When SCAP-deficient cells were incubated with either 25-HC or cholesterol, Insig-1 formed a complex with wild type SCAP (Fig. 4, *A*, *lanes 5* and *6*, and *B*, *lanes 2* and *3*) but not with SCAP containing the Y298C mutation (Fig. 4*B*, *lanes 5* and *6*). These data indicate that cholesterol and 25-HC are each capable of promoting complex formation between Insig and SCAP, provided that the crucial residues of SCAP that are required for its binding to Insig are not disrupted by mutation.

The above studies implicating the role of Insig proteins in the inhibitory effect of cholesterol and 25-HC on SREBP processing were carried out in transfected cells that overexpress Insigs and SCAP. To determine whether Insigs are required in nontransfected cells, we used RNA interference to knockdown simultaneously both Insig-1 and Insig-2 in SV-589 fibroblasts.

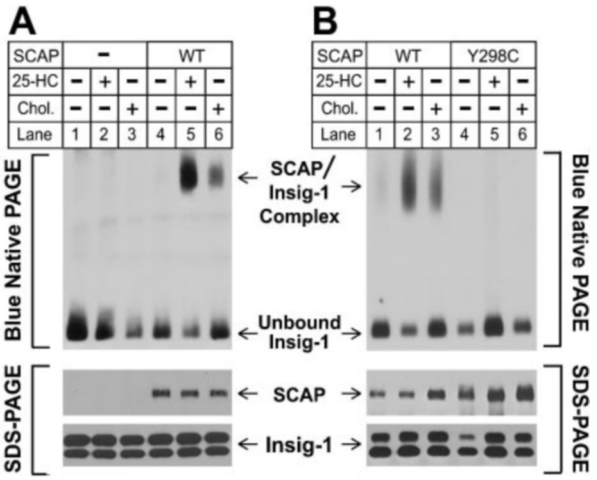

FIG. 4. **Stimulation of SCAP·Insig-1 complex formation by either 25-HC or cholesterol: Detection by blue native-PAGE.** SCAP-deficient SRD-13A cells were transfected with 0.05 μg of pCMV-Insig-1-Myc and 2 μg of TK-HSV-SREBP-2 in the absence or presence of either 1.25 μg of pCMV-SCAP or pCMV-SCAP(Y298C) as indicated. The cells were incubated in medium E for 1.5 h (*A*) or 1 h (*B*) and then for 6 h in medium D in the absence or presence of either 25 μM cholesterol/MCD or 2.5 μM 25-HC/MCD. Aliquots of the $1 \times 10^5 \times g$ membrane suspension were subjected to blue native-PAGE (*upper panel*) or SDS-PAGE (*middle* and *lower panels*). Immunoblot analysis was performed using anti-Myc IgG-9E10 for detection of Insig-1 (*upper* and *lower panels*) or anti-SCAP IgG-9D5 (*middle panel*). The filters were exposed to film for 15 s to 1 min.

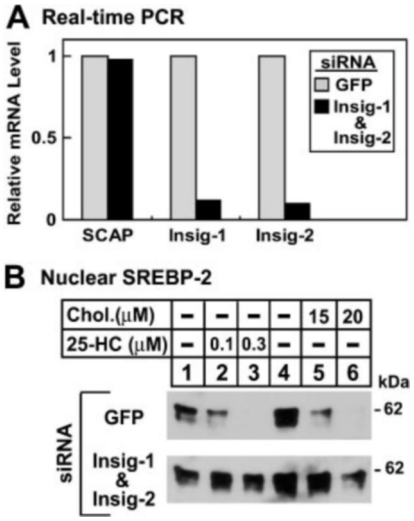

FIG. 5. **Effect of Insig knockdown on sterol-mediated suppression of SREBP-2 processing in human fibroblasts.** Human SV-589 fibroblasts were transfected with siRNA targeted against either green fluorescent protein or Insig-1 plus Insig-2 and used for experiments 3 days later as described under "Experimental Procedures." *A*, quantification of mRNA levels. One dish of cells was harvested for the total cellular RNA, which was subjected to quantitative real time PCR. The relative amount of mRNA in each condition was normalized to an internal control (cyclophilin) and compared with that of the cells transfected with the control siRNA (green fluorescent protein), which is arbitrarily set to a value of 1.0. *B*, immunoblot analysis of nuclear SREBP-2. Replicate dishes of cells were switched to medium F supplemented with 5% newborn calf lipoprotein-deficient serum, 50 μM compactin, 50 μM sodium mevalonate, and 1% hydroxypropyl-β-cyclodextrin. After incubation for 1 h at 37 °C, the cells were washed twice with PBS and switched to fresh medium F supplemented with 10% lipoprotein-deficient serum, 50 μM compactin, 50 μM mevalonate, and the indicated concentration of either 25-HC (*lanes 1–3*) or cholesterol (*lanes 4–6*) complexed to MCD. 75 min prior to harvest, *N*-acetyl-leucinal-leucinal-norleucinal was directly added to each dish at a final concentration of 25 μg/ml. After incubation for either 3 h (*lanes 1–3*) or 6 h (*lanes 4–6*), duplicate dishes of cells were harvested and pooled, and their nuclear extracts were immunoblotted with an antibody against human SREBP-2 (monoclonal IgG-1D2). The filters were exposed to film for 90 s.

RNAi treatment reduced the Insig-1 and Insig-2 mRNAs by ~85% as indicated by quantitative reverse transcriptase-PCR (Fig. 5*A*). In cells treated with a control double-stranded RNA directed against green fluorescent protein, 0.1 μM 25-HC reduced nuclear SREBP-2 after 3 h (Fig. 5*B*, *upper panel*, *lanes 1–3*). In the Insig-deficient cells, 25-HC did not reduce nuclear SREBP-2 even when added at a 3-fold higher level (Fig. 5*B*, *lower panel*, *lanes 1–3*). To study cholesterol regulation, it was necessary to extend the incubation period to 6 h (Fig. 5*B*, *lanes 4–6*). In the control cells the response to cholesterol showed a steep concentration dependence. There was a partial reduction of nuclear SREBP-2 at 15 μM cholesterol and a complete disappearance at 20 μM. In the Insig-deficient cells, this response curve was shifted to slightly higher values (Fig. 5*B*, *bottom panel*, *lanes 4–6*). Cholesterol at 15 μM had no detectable effect, and a partial response was seen at 20 μM. This partial resistance to cholesterol was observed in three other experiments in which both Insig-1 and Insig-2 mRNAs were reduced by RNAi treatment. The lack of complete resistance is likely attributable to the residual 15% of Insig-1 and Insig-2 mRNAs that remain in these cells. We were unable to check the levels of Insig-1 and Insig-2 proteins because antibodies that react with human Insigs are not yet available. We used human cells for these studies because they responded more briskly to RNA interference than did cells from other species. We note that the resistance to 25-HC was also partial in the RNAi-treated SV589 cells. In other experiments not shown, we observed a 50% suppression of SREBP cleavage when the 25-HC concentration was raised to 1 μM, even in the face of an 85% Insig deficiency.

Because both cholesterol and 25-HC inhibited SREBP processing and promoted SCAP·Insig complex formation in intact cells, we asked whether these sterols alter SCAP conformation under the same conditions. SCAP-deficient cells were transfected with SCAP and SREBP-2 in the absence and presence of Insig-1 and then incubated with cholesterol·MCD or 25-HC·MCD. Because of the SCAP overexpression, 25-HC does not block SREBP-2 processing unless Insig-1 or Insig-2 is overexpressed (11, 12). After incubation, the nuclear fractions were analyzed for SREBP-2 content (Fig. 6*A*, *lower panel*), and the membrane vesicles were subjected to limited proteolysis with trypsin to analyze SCAP conformation (Fig. 6*A*, *upper panel*). Both sterols blocked SREBP-2 processing, but only in the presence of excess Insig-1 (Fig. 6*A*). Cholesterol altered SCAP conformation, as revealed by an increase in the *lower band* in the SCAP digests (Fig. 6*A*, *lane 5*). 25-HC had no such effect (*lane 6*). The cholesterol-mediated conformational change in SCAP was also observed in the presence of Insig-2 (Fig. 6*B*). These results were quantitated by densitometry, and the results are shown graphically in Fig. 6*C*. These data indicate that 25-HC blocks SREBP-2 processing in a fashion that is dependent on Insig but does not involve a detectable conformational change in SCAP.

To further study the interaction of sterols with SCAP, we carried out cross-linking studies with 6-azi-5α-cholesterol-3β-ol (hereafter referred to as photocholesterol) (22). We also prepared the 25-hydroxylated derivative (designated photo 25-HC). Previous studies showed that photocholesterol mimics cholesterol in model membranes (33) and can substitute for cholesterol to allow growth and reproduction of *Caenorhabditis elegans* (34). Photocholesterol (Fig. 7*A*) and photo 25-HC can be activated by UV light, which breaks the diazirine ring and generates a carbene radical that cross-links covalently to interacting proteins (22). To efficiently deliver the photoactive sterols to membranes, both were complexed to MCD.

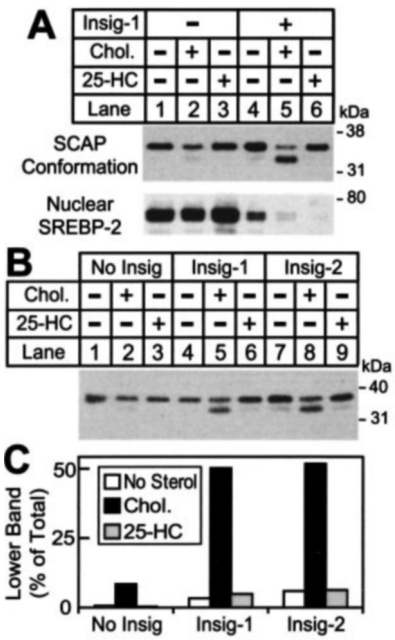

FIG. 6. **Insig-dependent alteration in trypsin digestion of SCAP after incubation of intact cells with cholesterol.** SCAP-deficient SRD-13A cells were transfected with 1.25 μg of pCMV-SCAP and 2 μg of TK-HSV-SREBP-2 in the absence or presence of 0.6 μg of pCMV-Insig1-Myc or 3 μg of pCMV-Insig2-Myc as indicated. After transfection, the cells were incubated for 2 h in medium E in the absence or presence of 50 μM of the indicated sterol complexed to MCD. The cells were then washed and harvested for preparation of membrane and nuclear fractions. *A* (*lower panel*), the content of cleaved SREBP-2 in the nuclear fraction was analyzed by immunoblot with anti-HSV-IgG. The filter was exposed to film for 30 s. *A* (*upper panel*) and *B*, aliquots of the 20,000*g* membrane suspension (100 μg) were sequentially treated with 2 μg of trypsin (30 °C for 30 min) and PNGase F. The samples were immunoblotted with IgG-9D5 (anti-SCAP). The filter was exposed to film for 60 s. *C*, relative intensities of the *upper* and *lower* bands in *B* were quantified by densitometry.

Fig. 7*B* shows that 50 μM photocholesterol and photo 25-HC both inhibited cleavage of endogenous SREBP-2 when added in MCD. As a negative control, we tested 5α-androsten-3β,17β-diol, which does not inhibit SREBP processing. We next tested whether photocholesterol would mimic the effect of cholesterol on SCAP conformation *in vitro*. The membranes were harvested from sterol-depleted cells expressing SCAP and Insig. Varying concentrations of cholesterol or photocholesterol were added to the membranes *in vitro*, followed by trypsin treatment to analyze SCAP conformation. Some membranes were exposed to UV after *in vitro* incubation with sterols but before trypsin treatment. In the absence of UV treatment, photocholesterol induced the conformational change in SCAP, with similar dose dependence as cholesterol, as indicated by the *lower band* in trypsin digests (Fig. 7, *C* and *D*). UV treatment had no effect on the response to cholesterol, but it enhanced the conformational change induced by photocholesterol, as illustrated by quantitative densitometry in Fig. 7*D*.

In the experiment of Fig. 7*C*, the UV-activated photocholesterol did not alter the electrophoretic mobility of either the 37- or 35-kDa SCAP fragments that were visualized after trypsin treatment. Inasmuch as these two trypsin-resistant fragments contain only the portion of SCAP that lies between the beginning of transmembrane helix 7 (TM 7) and the end of TM 8 (19), it is possible that photocholesterol is cross-linked to a different part of SCAP that is not detected by the IgG-9D5 antibody. To test this hypothesis, we added photocholesterol to membranes containing SCAP(TM1–6), a truncated protein that contains the sequence from the NH_2 terminus to the end of TM 6 (11). SCAP(TM1–6) contains the sterol-sensing domain (TM 2–6) of SCAP (8, 15) and retains the capacity to bind to Insig-1 in a sterol-dependent manner (11). The relatively small size of SCAP(TM1–6) (about 70 kDa) raised the possibility that we could detect a change in the electrophoretic mobility of the protein if it was cross-linked to photocholesterol, even without trypsin treatment. Accordingly, membranes containing SCAP(TM1–6) were incubated *in vitro* with sterols, then exposed to UV light, and analyzed by SDS-PAGE and immunoblot. Fig. 8 shows that photocholesterol (*lanes 6* and *8*) slowed the electrophoretic mobility of SCAP(TM1–6) in a UV-dependent manner, increasing the apparent molecular mass from 70 to 71 kDa. This mobility change is consistent with cross-linking of photocholesterol to SCAP(TM1–6). The effect was specific for SCAP(TM1–6), because photocholesterol did not alter the electrophoretic mobility of Insig-1, which appears as two bands of 37 and 40 kDa (11). In contrast to photocholesterol, photo 25-HC did not alter the electrophoretic mobility of SCAP(TM1–6) (*lane 10*).

To localize the region within SCAP (TM1–6) that cross-links to photocholesterol, we transfected cells with a plasmid encoding full-length SCAP with an HSV epitope tag at the NH_2 terminus (Fig. 9*A*). For comparative purposes, we transfected cells with a plasmid encoding full-length SCAP without the HSV tag. We isolated membranes, solubilized the proteins with Triton X-100, performed a partial digest with chymotrypsin, and subjected aliquots of the digests to SDS-PAGE on 8% polyacrylamide gels to visualize high M_r proteins (Fig. 9*B*, *upper panel*) or 15% polyacrylamide to visualize low M_r fragments (Fig. 9*B*, *lower panel*). In the absence of chymotrypsin treatment, immunoblotting with IgG-9D5, the antibody against the loop between TM7 and TM8, revealed that the HSV epitope tag increased the apparent molecular mass of the full-length SCAP (compare *lanes 1* and *3*, *upper panel*). Because the digestions were conducted in detergent, the IgG-9D5 epitope was destroyed by chymotrypsin (*lanes 2* and *4*, *upper* and *lower panels*). Immunoblotting with anti-HSV revealed the full-length protein in the absence of chymotrypsin (*lane 7*, *upper panel*). Even in the presence of detergent, the HSV epitope was not destroyed by chymotrypsin as shown by immunoblotting with anti-HSV, which revealed a fragment with a mobility corresponding to a molecular mass of 10 kDa (*lane 8*, *lower panel*, indicated by *arrow*). We estimate that this fragment encompasses amino acids 1 to ~64 in SCAP (plus the HSV tag). This fragment would include the first membrane-spanning segment and about 20% of the first luminal loop of SCAP.

To determine whether photocholesterol cross-links to the 10-kDa NH_2-terminal fragment, we isolated membranes from cells expressing the HSV-tagged construct, exposed the membranes to photocholesterol, and irradiated with UV light. To confirm that the photocholesterol caused a conformational change in SCAP, one aliquot of membranes was treated with trypsin in the absence of detergent, then treated with PNGase F to remove carbohydrate, and blotted with IgG-9D5 to visualize the protected fragment between TM7 and TM8 (Fig. 9*C*, *lower panel*). Another aliquot of membranes was solubilized with Triton X-100, treated with chymotrypsin, subjected to electrophoresis in 15% polyacrylamide, and blotted with anti-HSV (Fig. 9*C*, *upper panel*). Cholesterol and photocholesterol, but not photo 25-HC, caused a conformational change in SCAP, as revealed by the appearance of the lower band after trypsin digestion of intact vesicles (Fig. 9*C*, *lower panel*). In the chymotrypsin digests, the addition of photocholesterol at 30 or 50 μM caused a retarded migration of the 10-kDa fragment (Fig. 9*C*, *upper panel*, *lanes 6* and *8*). This change was seen only after UV irradiation, and it was not

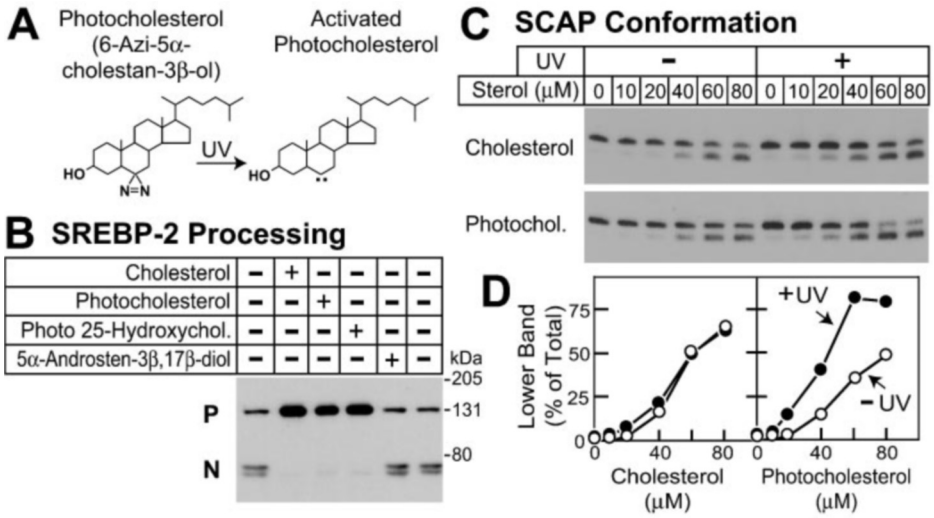

FIG. 7. **Effect of photocholesterol on SREBP-2 processing and SCAP conformation.** *A*, structure of photocholesterol before and after activation by UV. *B*, immunoblot analysis of SREBP-2. CHO K1 cells were incubated for 2 h in medium E in the absence or presence of 50 μM of the indicated sterol complexed to MCD. Total cell extracts were prepared and immunoblotted with IgG-7D4 (anti-SREBP-2). The filter was exposed to film for 45 s. *C*, trypsin digestion of SCAP. SCAP-deficient SRD-13A cells were transfected with 2 μg of pCMV-SCAP, 0.3 μg of pCMV-Insig1-Myc, and 2 μg of pTK-HSV-SREBP-2. The cells were incubated in medium D in the absence of sterols for 16 h. Aliquots of the 20,000 × *g* membrane suspension were sequentially incubated for 20 min at room temperature with the indicated concentration of sterol complexed to MCD, centrifuged at 20,000 × *g* for 10 min at 4 °C, resuspended in buffer A, and incubated for 10 min on ice in the absence or presence of UV light. SCAP conformation was then analyzed by trypsin treatment as described for Fig. 6. The filter was exposed to film for 45 s. *D*, relative intensities of the *upper* and *lower* bands in *C* were quantified by densitometry.

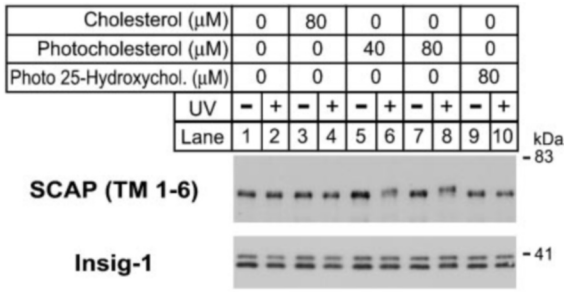

FIG. 8. **Specific cross-linking of photocholesterol to the membrane domain of SCAP.** Membrane suspensions (20,000 × *g* fraction) were prepared from SCAP-deficient SRD-13A cells transfected with 4 μg of pCMV-SCAP(TM1–6)-Myc plus 0.25 μg of pCMV-Insig1-Myc. Aliquots of the membrane suspensions were incubated with the indicated concentration of sterol complexed to MCD and treated with UV light as described under "Experimental Procedures." The samples were immunoblotted with anti-Myc IgG-9E10. The filters were exposed to film for 30 s (*upper*) or 3 s (*lower*).

observed with cholesterol or photo 25-HC. These data indicate that photocholesterol cross-links to the region of SCAP containing the first transmembrane segment.

We next sought to determine whether photocholesterol cross-links to SCAP in intact cells. For this purpose, cells expressing HSV-SCAP were treated with various sterols in MCD, and selected dishes were exposed to UV irradiation prior to homogenization. The isolated membrane fraction was solubilized with Triton X-100, digested with chymotrypsin, and blotted with anti-HSV to visualize the NH_2-terminal 10-kDa fragment. We also isolated a nuclear pellet from the same cells and measured the content of processed SREBP-2 by immunoblotting. The data show that photocholesterol cross-linked to the NH_2-terminal fragment of SCAP in intact cells, as indicated by the retarded band in Fig. 9*D* (*upper panel*, *lane 7*). This cross-linking was dependent on UV irradiation, and it was not seen with cholesterol or with photo 25-HC. All three sterols entered the cells as indicated by the observation that all three blocked SREBP-2 processing (Fig. 9*D*, *lower panel*).

DISCUSSION

The current data on sterol regulation in intact cells resolve a long standing ambiguity in this field. They demonstrate that cholesterol and an oxysterol such as 25-HC both inhibit SREBP cleavage by inducing the escort protein, SCAP, to bind to Insigs, but they do so by different mechanisms. Cholesterol binds directly to SCAP and induces a conformational change, whereas 25-HC does not. These experiments were made possible through the use of MCD as a vehicle to deliver sterols to cells. When delivered to intact cells in this manner, cholesterol and 25-HC both inhibited SREBP cleavage (Fig. 1). A similar inhibition was observed with photoactivatable derivatives of the two sterols (Fig. 7*B*). When exposed to UV light, photocholesterol became cross-linked to the TM1–6 portion of SCAP as demonstrated by the retarded electrophoretic mobility of the protein, but photo 25-HC failed to cross-link (Fig. 8). Binding of cholesterol or photocholesterol to SCAP in intact cells induced a conformational change that persisted when membrane vesicles were isolated and digested *in vitro* with trypsin (Figs. 6, 7, and 9). The size of the cholesterol-induced tryptic fragment was consistent with the exposure of arginine 503, the same arginine that becomes exposed to trypsin when cholesterol is added to cell membranes *in vitro* (16, 19). Arginine 503 did not become exposed when 25-HC was added to cells (Fig. 6), nor was it exposed when 25-HC was added to membranes in earlier experiments (16). Even though 25-HC failed to interact with SCAP directly, it still induced SCAP to bind to Insigs, as revealed by altered migration of the complex on blue native gel electrophoresis (Fig. 4). Considered together, these findings strongly suggest that 25-HC must interact with an unidentified protein whose action induces SCAP to bind Insigs.

Limited proteolysis studies showed that photocholesterol was covalently attached to a region of SCAP that contains the cytoplasmic NH_2 terminus, TM1, and a portion of the first ER luminal loop. Cross-linking to this site occurred both *in vitro* (Fig. 9*C*) and in intact cells (Fig. 9*D*) and correlated with the conformational change in SCAP and suppression of SREBP-2 processing. Notably, this site of photocholesterol cross-linking

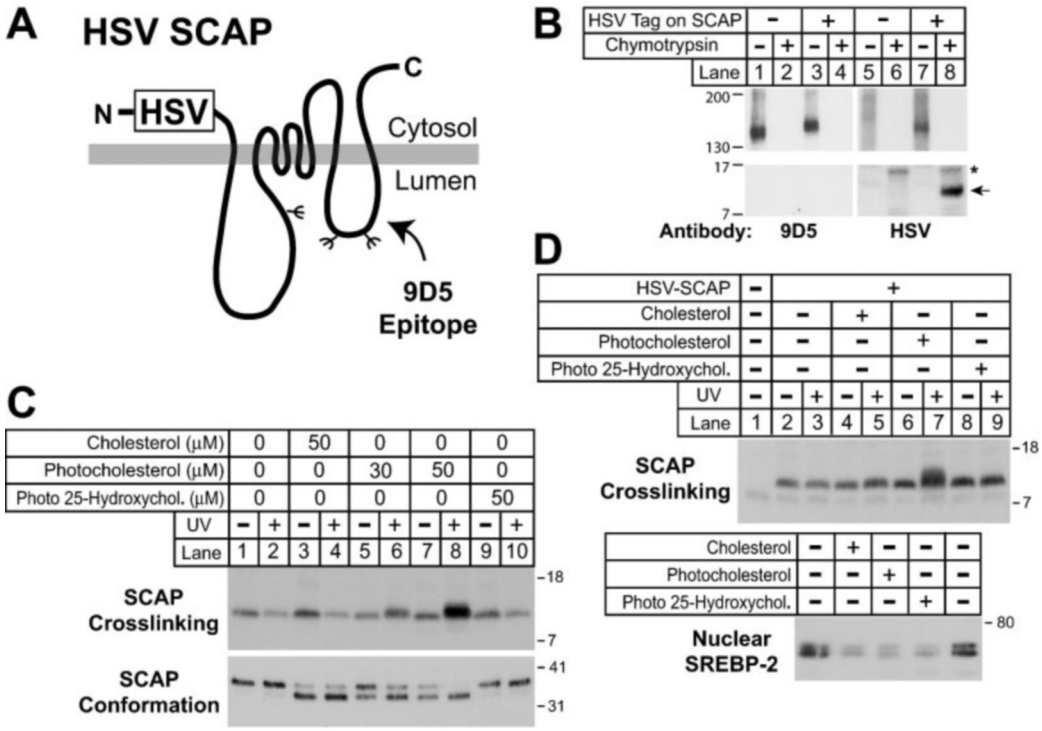

FIG. 9. **Localization of cross-linked photocholesterol to the first transmembrane segment of SCAP.** *A*, proposed membrane topology of SCAP, showing location of the NH_2-terminal HSV epitope tag, the epitope recognized by IgG-9D5, and the *N*-glycosylation sites. *B*, chymotrypsin digestion of HSV-tagged SCAP. SCAP-deficient SRD-13A cells were transfected with 0.5 μg of pCMV-Insig1-Myc and either 2 μg of pCMV-SCAP (*lanes 1*, *2*, *5*, and *6*) or 2 μg of pTK-HSV-SCAP (*lanes 3*, *4*, *7*, and *8*). The cells were incubated in medium E for 2 h, and aliquots of the 20,000 × *g* membrane suspension (100 μg) were incubated at 30 °C for 30 min in the absence or presence of 30 μg chymotrypsin plus 1% (v/v) Triton X-100. The samples were subjected to SDS-PAGE on either an 8% Tris-glycine gel (*upper*) or a 15% Tris-Tricine gel (*lower*) and then immunoblotted for SCAP using either IgG-9D5 or anti-HSV IgG. The filters were exposed to film for 1 min. The *asterisk* denotes a nonspecific band. *Arrow* denotes NH_2-terminal fragment of HSV-SCAP. *C*, localization of photocholesterol cross-link to TM1 of SCAP and its effect on SCAP conformation. SRD-13A cells were transfected with 4 μg of pTK-HSV-SCAP and 0.5 μg of pCMV-Insig1-Myc. The cells were incubated for 2 h in medium E without sterols. Aliquots of the 20,000 × *g* membrane suspension were incubated with the indicated concentration of the indicated sterol·MCD complex *in vitro* and treated with UV light as described under "Experimental Procedures." The samples were then treated for 30 min at 30 °C with either chymotrypsin plus 1% Triton X-100 or trypsin without Triton X-100. Chymotrypsin-treated samples (*upper panel*) were immunoblotted for SCAP using anti-HSV IgG. Trypsin-treated samples (*lower panel*) were treated with PNGase F before immunoblot analysis for SCAP using IgG-9D5. The filters were exposed to film for 1 min. *D*, photocholesterol cross-linking to TM1 of SCAP and its effect on SREBP-2 processing in intact cells. SRD-13A cells were transfected with 2 μg of pTK-HSV-SREBP-2 and 0.3 μg of pCMV-Insig1-Myc in the absence or presence of 1.25 μg pTK-HSV-SCAP as indicated. The cells were incubated for 2 h in medium E in the absence or presence of 50 μM of the indicated sterol·MCD complex, irradiated for 20 min as described under "Experimental Procedures," and then harvested for preparation of nuclear and membrane fractions. Aliquots of the 20,000 × *g* membrane suspension were treated with chymotrypsin plus 1% Triton X-100 and immunoblotted for SCAP using anti-HSV IgG (*upper panel*). The content of cleaved SREBP-2 in the nuclear fraction was analyzed by immunoblot with anti-HSV-IgG (*lower panel*). The filters were exposed to film for 15 s.

lies outside TM2–6, which was previously defined as the sterol-sensing domain based on primary sequence homology between several proteins involved in cholesterol homeostasis (8, 15). Photocholesterol cross-links to SCAP through a carbene radical at the C-6 position of cholesterol. Inasmuch as this carbene can form covalent bonds nonspecifically with various residues on SCAP, the cross-linking of photocholesterol to the NH_2-terminal position of SCAP may not reflect a direct interaction of cholesterol with this specific region of the molecule. It only indicates that TM1 is within close proximity to the true cholesterol-binding site. This binding site may well reside in the sterol-sensing domain.

The current data indicate that 25-HC and cholesterol induce SCAP·Insig binding by different mechanisms, and they contradict an earlier suggestion that 25-HC may act by causing cholesterol to translocate to the ER membrane where it would bind to SCAP (16, 19). If this were the case, then 25-HC should have induced a conformational change in SCAP when added to intact cells. This was clearly not the case as illustrated by the trypsin digestion pattern of SCAP isolated from 25-HC-treated cells (Fig. 6, *A* and *B*).

Using MCD as a delivery vehicle, we tested the structural features of cholesterol that are required for regulation of SREBP processing *in vivo* (Fig. 2) and found a strong correlation with the structural requirements for sterol binding to purified recombinant SCAP *in vitro* (15). Most remarkably, the isooctyl side chain was not required for regulation of processing (*i.e.* 5-androsten-3β-ol was active), and the Δ5-double bond was dispensable. The stereochemistry at the 3-position was crucial; the 3β-hydroxyl group was effective, but the 3α derivative (as in epicholesterol) was not. Likewise, in the previous *in vitro* binding studies, SCAP failed to bind epicholesterol with high affinity, but it did bind 5-androsten-3β-ol (15). The activity of 5-androsten-3β-ol was eliminated in intact cells (Fig. 2) and in membranes (15) when an additional hydroxyl group was added at the 17β-position. These findings suggest that the sterol-binding site on SCAP must interact with the 3β-hydroxyl group of cholesterol. Accessibility to this binding site is hindered when a polar group is present at the other end of the molecule, either on the D ring or at the 25-position. One possibility is that polarity on the side chain prevents a sterol from inserting into membranes or detergent micelles in a configuration that permits it to bind to SCAP. This access problem may explain why cells need the postulated 25-HC-binding protein for 25-HC to regulate SREBP cleavage.

In this paper, as in previous studies from this laboratory,

sterol-mediated regulation was crucially dependent on the relative amounts of SCAP and Insigs. In transfected cells that express an excess of SCAP relative to Insigs, neither cholesterol nor 25-HC will inhibit SREBP processing (Fig. 6*A*, *lanes 1–3*). Moreover, under these conditions cholesterol does not cause a conformational change in SCAP (Fig. 6*B*, *lanes 1–3*). Concomitant overexpression of Insig-1 or Insig-2 restores both aspects of sterol function (Fig. 6, *A-C*). At intermediate ratios of SCAP to Insigs, partial resistance to sterols is observed. On the other hand, if Insigs are expressed at levels that are too high, SREBP processing is blocked even when no sterols are added (11), perhaps because SCAP becomes sensitive to the low levels of endogenous sterols that are present even in sterol-depleted cells. These data indicate that Insigs modulate the cholesterol-induced conformational change in SCAP, perhaps by stabilizing the SCAP·cholesterol complex. Because of this interdependence, whenever we prepare a new batch of plasmids for transfection, we perform preliminary titration curves of the SCAP and Insig plasmids to find the ratio that gives the most complete sterol regulation. The plasmids are then stored and used repeatedly for experiments. This difference in SCAP·Insig ratios may explain why untransfected CHO K1 cells are more sensitive to cholesterol and 25-HC (Figs. 1 and 2) than are the SCAP-deficient SRD-13A cells that are used for experiments requiring transfection (Figs. 7–9).

Although the current results suggest the existence of a 25-HC-responsive regulatory protein, the nature of this putative protein is unclear. In the mid 1980s, Taylor and Kandutsch (35) described and our laboratory isolated and cloned (36, 37) a 25-HC-binding protein from hamster liver cytosol. We designated this protein as oxysterol-binding protein (OSBP) (36, 38), and it is now referred to as OSBP-1. This protein is the founding member of a superfamily that includes 15 OSBP-related molecules in mammalian genomes (39). Immunofluorescence studies revealed that OSBP-1 translocated from the cytosol to the Golgi when 25-HC was added to cultured cells (40). OSBP-1 contains a pleckstrin homology domain that is responsible for this translocation. OSBP-1 was subsequently shown to modulate the activity of βARK, a kinase that phosphorylates β-adrenergic receptors (41).

In multiple experiments, our laboratory has never been able to find evidence that OSBP-1 was involved in 25-HC-mediated regulation of cholesterol metabolism or SREBP processing. Thus, massive overexpression of OSBP-1 by cDNA transfection did not influence the SREBP response to 25-HC. Moreover, overexpression of the sterol-binding domain or the pleckstrin homology domain of OSBP failed to have a dominant-negative effect on regulation of SREBP processing. We also attempted to reduce expression of OSBP-1 by RNA interference. Although we reduced the OSBP-1 mRNA level by 90% and simultaneously reduced its closest paralog, ORP-4, by 80%, we did not affect the response to 25-HC.[2]

It is possible that the true 25-HC sensor is not OSBP-1 but rather one of the 15 OSBP-related proteins whose cDNAs have been sequenced (39). Studies are now under way to document the existence and determine the identity of the postulated 25-HC regulatory protein.

[2] C. M. Adams, J. D. Feramisco, L. Li, M. S. Brown, and J. L. Goldstein, unpublished observations.

Acknowledgments—We thank our colleagues Arun Radhakrishnan and David Russell for helpful comments, Debra Morgan for technical assistance, and Lisa Beatty and Angela Carroll for invaluable help with tissue culture.

REFERENCES

1. Kandutsch, A. A., and Chen, H. W. (1974) *J. Biol. Chem.* **249,** 6057–6061
2. Brown, M. S., and Goldstein, J. L. (1974) *J. Biol. Chem.* **249,** 7306–7314
3. Goldstein, J. L., Faust, J. R., Brunschede, G. Y., and Brown, M. S. (1975) in *Lipids, Lipoproteins, and Drugs* (Kritchevsky, D., Paoletti, R., and Holmes, W. L., eds) pp. 77–84, Plenum, New York
4. Kandutsch, A. A., Chen, H. W., and Heiniger, H.-J. (1978) *Science* **201,** 498–501
5. Goldstein, J. L., and Brown, M. S. (1974) *J. Biol. Chem.* **249,** 5153–5162
6. Krieger, M., Goldstein, J. L., and Brown, M. S. (1978) *Proc. Natl. Acad. Sci. U. S. A.* **75,** 5052–5056
7. Brown, M. S., and Goldstein, J. L. (1986) *Science* **232,** 34–47
8. Brown, M. S., and Goldstein, J. L. (1999) *Proc. Natl. Acad. Sci. U. S. A.* **96,** 11041–11048
9. Goldstein, J. L., Rawson, R. B., and Brown, M. S. (2002) *Arch. Biochem. Biophys.* **397,** 139–148
10. Horton, J. D., Goldstein, J. L., and Brown, M. S. (2002) *J. Clin. Invest.* **109,** 1125–1131
11. Yang, T., Espenshade, P. J., Wright, M. E., Yabe, D., Gong, Y., Aebersold, R., Goldstein, J. L., and Brown, M. S. (2002) *Cell* **110,** 489–500
12. Yabe, D., Brown, M. S., and Goldstein, J. L. (2002) *Proc. Natl. Acad. Sci. U. S. A.* **99,** 12753–12758
13. Feramisco, J. D., Goldstein, J. L., and Brown, M. S. (2003) *J. Biol. Chem.* **279,** 8487–8496
14. Yabe, D., Xia, Z.-P., Adams, C. M., and Rawson, R. B. (2002) *Proc. Natl. Acad. Sci. U. S. A.* **99,** 16672–16677
15. Radhakrishnan, A., Sun, L.-P., Kwon, H. J., Brown, M. S., and Goldstein, J. L. (2004) *Mol. Cell* **15,** 259–268
16. Adams, C. M., Goldstein, J. L., and Brown, M. S. (2003) *Proc. Natl. Acad. Sci. U. S. A.* **100,** 10647–10652
17. Kilsdonk, E. P. C., Yancey, P. G., Stoudt, G. W., Bangerter, F. W., Johnson, W. J., Phillips, M. C., and Rothblat, G. H. (1995) *J. Biol. Chem.* **270,** 17250–17256
18. Sakai, J., Nohturfft, A., Cheng, D., Ho, Y. K., Brown, M. S., and Goldstein, J. L. (1997) *J. Biol. Chem.* **272,** 20213–20221
19. Brown, A. J., Sun, L., Feramisco, J. D., Brown, M. S., and Goldstein, J. L. (2002) *Mol. Cell* **10,** 237–245
20. Goldstein, J. L., Basu, S. K., and Brown, M. S. (1983) *Methods Enzymol.* **98,** 241–260
21. Brown, M. S., Faust, J. R., Goldstein, J. L., Kaneko, I., and Endo, A. (1978) *J. Biol. Chem.* **253,** 1121–1128
22. Thiele, C., Hannah, M. J., Fahrenholz, F., and Huttner, W. B. (2000) *Nat. Cell Biol.* **2,** 42–49
23. Tavares, R., Randoux, T., Braekman, J.-C., and Daloze, D. (1993) *Tetrahedron* **49,** 5079–5090
24. Hua, X., Sakai, J., Brown, M. S., and Goldstein, J. L. (1996) *J. Biol. Chem.* **271,** 10379–10384
25. Nohturfft, A., Brown, M. S., and Goldstein, J. L. (1998) *J. Biol. Chem.* **273,** 17243–17250
26. Rawson, R. B., DeBose-Boyd, R. A., Goldstein, J. L., and Brown, M. S. (1999) *J. Biol. Chem.* **274,** 28549–28556
27. Yamamoto, T., Davis, C. G., Brown, M. S., Schneider, W. J., Casey, M. L., Goldstein, J. L., and Russell, D. W. (1984) *Cell* **39,** 27–38
28. DeBose-Boyd, R. A., Brown, M. S., Li, W.-P., Nohturfft, A., Goldstein, J. L., and Espenshade, P. J. (1999) *Cell* **99,** 703–712
29. Liang, G., Yang, J., Horton, J. D., Hammer, R. E., Goldstein, J. L., and Brown, M. S. (2002) *J. Biol. Chem.* **277,** 9520–9528
30. Yang, J., Brown, M. S., Ho, Y. K., and Goldstein, J. L. (1995) *J. Biol. Chem.* **270,** 12152–12161
31. Shimano, H., Horton, J. D., Hammer, R. E., Shimomura, I., Brown, M. S., and Goldstein, J. L. (1996) *J. Clin. Invest.* **98,** 1575–1584
32. Russell, D. W. (2003) *Annu. Rev. Biochem.* **72,** 137–174
33. Mintzer, E. A., Waarts, B.-L., Wilschut, J., and Bittman, R. (2002) *FEBS Lett.* **510,** 181–184
34. Matyash, V., Geier, C., Henske, A., Mukherjee, S., Hirsh, D., Thiele, C., Grant, B., Maxfield, F. R., and Kurzchalia, T. V. (2001) *Mol. Biol. Cell* **12,** 1725–1736
35. Taylor, F. R., and Kandutsch, A. A. (1985) *Chem. Phys. Lipids* **38,** 187–194
36. Dawson, P. A., Ridgway, N. D., Slaughter, C. A., Brown, M. S., and Goldstein, J. L. (1989) *J. Biol. Chem.* **264,** 16798–16803
37. Dawson, P. A., van der Westhuyzen, D. R., Goldstein, J. L., and Brown, M. S. (1989) *J. Biol. Chem.* **264,** 9046–9052
38. Levanon, D., Hsieh, C.-L., Francke, U., Dawson, P. A., Ridgway, N. D., Brown, M. S., and Goldstein, J. L. (1990) *Genomics* **7,** 65–74
39. Olkkonen, V. M. (2004) *Curr. Opin. Lipidol.* **15,** 321–327
40. Ridgway, N. D., Dawson, P. A., Ho, Y. K., Brown, M. S., and Goldstein, J. L. (1992) *J. Cell Biol.* **116,** 307–319
41. Touhara, K., Inglese, J., Pitcher, J. A., Shaw, G., and Lefkowitz, R. J. (1994) *J. Biol. Chem.* **269,** 10217–10220